Experiments on rotating flows: impact of rotation on flow through tilted rectangular ducts

Leo R.M. Maas
Royal Netherlands Institute for Sea Research (NIOZ)
PO Box 59, 1790 AB Texel, the Netherlands
maas@nioz.nl
and
Institute for Marine and Atmospheric research Utrecht (IMAU)
Utrecht University, the Netherlands

Abstract:

In nature, flows can turn unstable and generate waves. Depending on circumstances, these waves may in turn retard or accelerate these flows. The importance of rotation on this process is studied. This is done by pumping fluid through a rectangular duct that is put on a rotating platform, and by measuring, for given pump and rotation rates, cross-channel pressure difference as well as through flow. As the flow passes the rigid-lid duct, instabilities develop that lead to inertial waves. Depending on a lateral tilt of the duct, these waves may or may not be focused onto a simple-shaped wave attractor, which may impact the through flow.

Key-words: inertial waves; wave attractor; fluid experiments

1 Introduction

When by subjecting a fluid to a pressure head, a flow is pumped through a container – a duct, is rotation going to aid the through flow or obstruct it? Naively one expects that rotation leads to additional drag on the fluid motion. Energy is needed not only to support the secondary circulation set-up by Ekman fluxes in horizontal boundary layers which appears in the form of streamwise tubes of two or four cell structure (Nandakumar, Raszillier and Durst 1991), but also to support the turbulence resulting from centrifugal, Ekman layer and other instabilities of the sheared through-flow (Greenspan 1968, Finlay 1992). When the rotation rate increases, all of this should lead to an increased pressure drop in the down-channel direction, which, in other words, is sensed as increased friction (Mårtensson et al 2002, Pallares, Grau and Davidson, 2005). Remarkably, there are cases when the pressure drop does however *not* seem to grow with increasing rotation rate (Dobner 1959). This suggests that the answer to our question is more subtle, and that, in fact, rotation may perhaps facilitate an *increasing* flow rate. The reason for this might lie in the fate of the aforementioned instabilities. In a three-dimensional, non-rotating fluid, instabilities will bring energy to the smallest scale through a process of nonlinear interactions. At these smallest scales, energy is degraded into heat. Rotation, however, leads to an *inverse* energy cascade supporting the *largest* (basin-scale) motions as it suppresses radial motion. This suppression of radial motion is caused by a radial stratification in angular momentum that presents the fluid with an apparent two-dimensionality, akin to that of a density-stratified fluid in a field of gravity. This type of stratification is stable as long as the angular momentum increases radially outwards (Rayleigh's criterion) and endows the fluid with elasticity, supporting inertial waves (Greenspan 1968). These waves propagate throughout the fluid, up to the container scale, which for the basin-scale waves takes place within one rotation period (Morize and Moisy 2006, Bewley et al. 2007, Messio et al. 2007). Thus, when instability ('turbulence') manifests itself, it will likely be, to some extent at least, in the form of inertial waves. This may completely change the cascading of energy; the energy transfer no longer necessarily evolves through nonlinear interactions, but might as well proceed through the re-

organization brought about by multiply-reflecting inertial waves (see Davidson, Staplehurst and Dalziel 2007). It thus becomes of interest to consider the fate of these inertial waves. Do the waves spread ergodically through the container, thus eventually again loosing their energy due to internal friction and upon reflection at boundaries? Or, do the waves organize themselves, e.g. in forming eigenmodes, *i.e.* spatially standing waves (Maas 2003)? It appears, perhaps somewhat surprisingly, that the *shape and orientation* of the container may play an important role here, as it turns out to be important whether the container shape is breaking the symmetry imposed by rotation, or not. Phillips (1963) first showed how linear inertial waves that reflect from an inclined wall change their wave number. This is due to the peculiar dispersion relation that these waves satisfy, which is scale-free. The frequency only relates to the wave vector *direction*, not to its magnitude. As the wave frequency is unaltered upon reflection of the wave, so is its angle with respect to the rotation axis. But, in order to satisfy the impermeability constraint at the solid boundary, the wave number changes. In other words, the waves focus or defocus, which is accompanied by either an amplification or reduction of energy density (current speed), respectively. In a confined domain (such as any real fluid needs for its containment) focusing dominates (Maas and Lam 1995). For almost any container shape, at least in two dimensions, wave energy appears to collect on a limit cycle, called *wave attractor* (see review in Maas 2005). This is a well-defined orbit (see Fig. 1) whose location is determined by the geometry and by the ratio of wave frequency, ω, to inertial frequency, 2Ω, where Ω is the frame's rotation rate. It is on approach of this wave attractor that the inertial waves turn unstable and mix fluid differing in angular momentum. In a laboratory experiment this was observed to set up a (cyclonic) mean flow (Maas 2001) that might in the present experiment actually amplify also the through flow. This suggests that, while the wave attractor

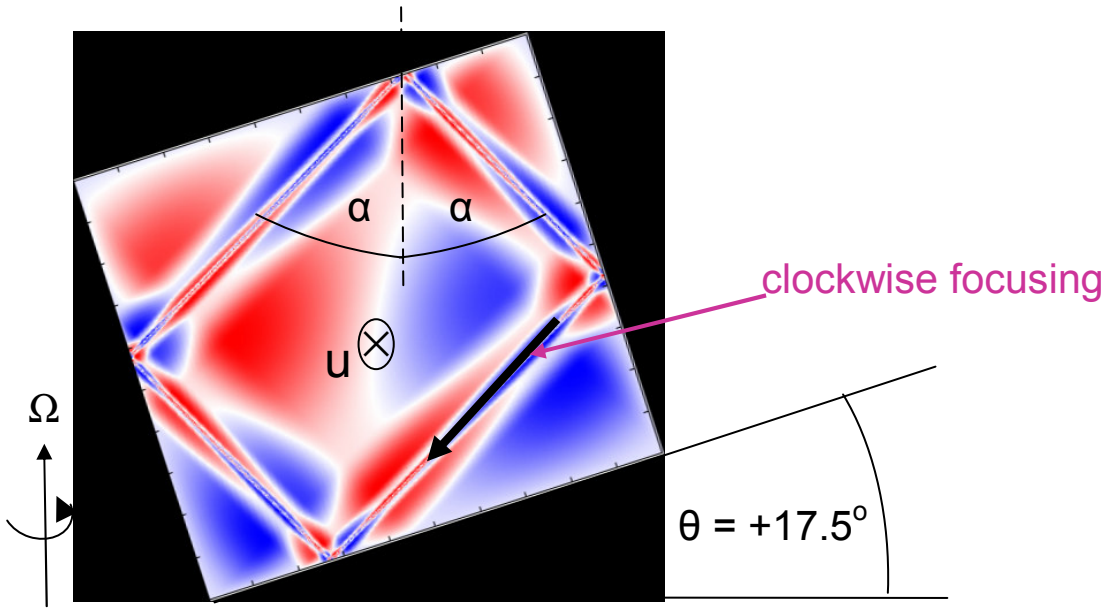

Fig. 1 Example of a wave attractor: the rectangular shape visible in the streamfunction field (colors), of focused inertial waves of frequency $\omega/2\Omega = \sin\alpha = 0.657$ that occurs in an infinitely long, tilted rectangular channel (tilt $\theta = 17.5^o$). Side view kindly supplied by S. Kopecz, and computed using the web method of Maas and Lam (1995). The orientation of the four 'limbs' of the attracting rectangle betrays the underlying web of characteristics that maintain a fixed direction $\alpha = 42.5^o$, relative to the rotation axis as determined by the dispersion relation (see Fig. 2b). The imposed through flow, whose instabilities should give rise to the inertial waves, is designated by ***u*** *and points into the paper.*

presents an extra *internal* boundary layer, this does not necessarily lead to a degradation of energy into heat, but rather seems to transfer energy to the mean field via a process of inertial wave breaking and rectification as found in related studies (Thompson 1970, McGuinness, Boyer and Fernando 2001).

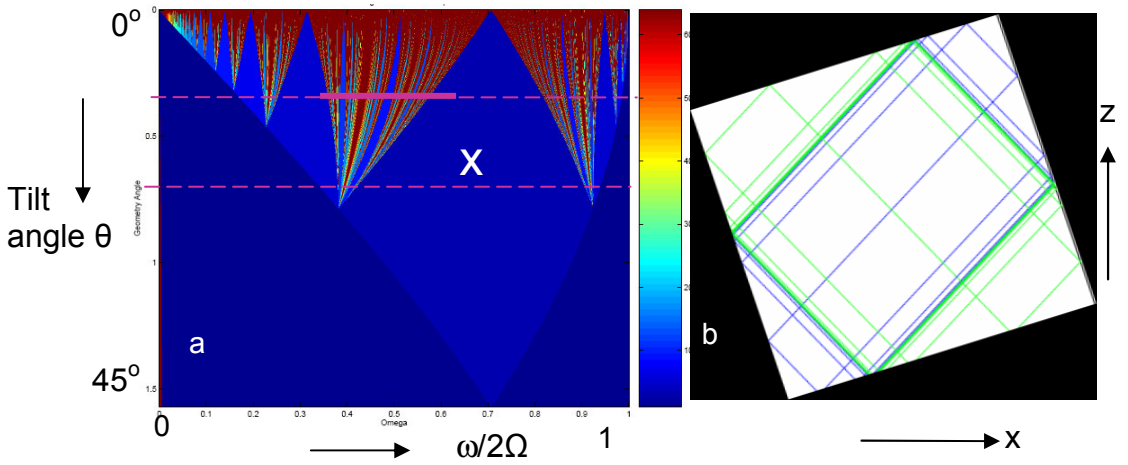

Fig. 2 (a) Length of the wave attractor (limit cycle) of titled square duct (color) as a function of tilt angle θ and ratio of wave frequency ω and inertial frequency 2 Ω, taken from Swart (2007). Dashed lines indicate tilts used in the experiments. Solid line segment is discussed in text. (b) Example of characteristic paths and rectangular wave attractor for particular conditions used in Fig. 1, the white cross in (a).

Wave attractors can be characterized by the length of their periodic orbit. Fig. 2a displays this length as a function of tilt angle θ and ratio $\omega/2\Omega = \sin\alpha$, related to angle to the vertical α. This plot is characterized by large areas of nearly equal attractor length, ranging from short (bright blue) to long (red). [Dark blue indicates that a corner point, of 'length' zero, is attracting.] Fig. 2a shows that the attractor length has a fractal distribution (analogous to the Lyapunov exponent in Maas et al 1997), which betrays the presence of so-called Arnold' tongues. In Fig.2a's central blue area (where also Figs. 1 and 2b are taken from, see white cross), the periodic orbit is simply a rectangle. In homogeneous rotating fluids, wave attractors have experimentally been found in a trapezoidal container (Maas 2001, Manders and Maas 2003, 2004). In these cases, waves were excited by purposely introducing a single perturbation frequency by weak modulation of background rotation rate Ω. An experimental confirmation for the existence of a wave attractor in a tilted box of square cross-section, forced in a similar manner for parameter values close to those used in the examples of Figs. 1 and 2b, is given in Fig. 3a. Despite the box being obviously of finite length in the real experiment, the current speed clearly shows the nearly square shape of the wave attractor corresponding to the forcing frequency. This compares well with the shape computed by Ogilvie (2005) for the analogous case of a wave attractor in a viscous, stratified, non-rotating fluid in a tilted square domain (Fig. 3b).

While their excitation might not be as clear cut in rotating flows, the aim of the present contribution is to present a number of fluid experiments in which a broad-band spectrum of inertial waves may yet be relevant to the through flow such as measured here as a function of imposed rotation and flow rates. Significant findings are observations of a fast rotating geostrophic regime, where inertial and Rossby waves dominate, and a slowly rotating turbulent regime. The possible role of the inertial waves in amplifying the through flow, by generating a

wave attractor, is addressed. Only preliminary results will be reported here. A more comprehensive discussion awaits further analysis.

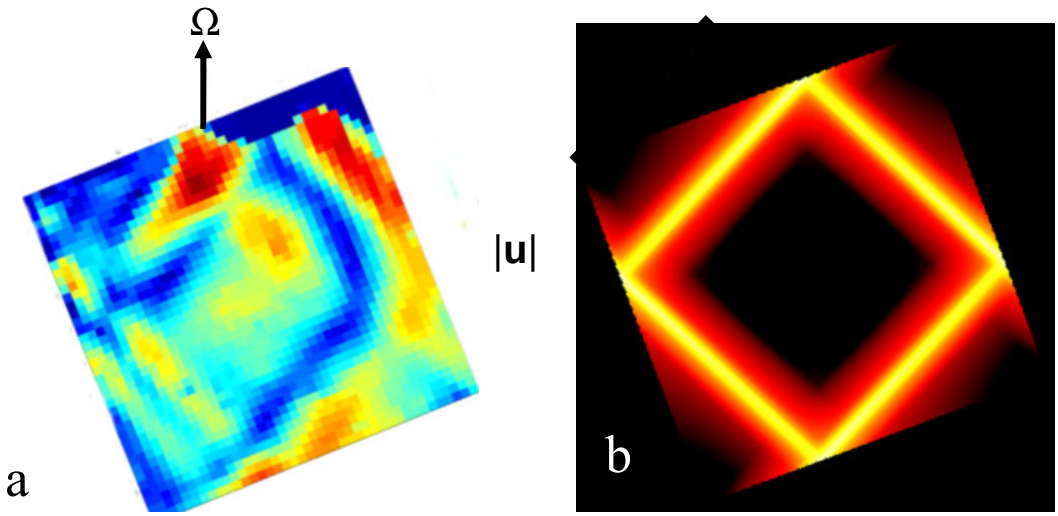

Fig. 3 (a) Experimental confirmation of existence of inertial wave attractor in tilted box of square cross-section (Manders and Maas, unpublished ms). Notice that the blue area at the top indicates absence of scatterers (due to sinking). These scatterers are used in the Particle Image Velocimetry method employed to visualize the currents, of which the speed, $|\boldsymbol{u}|$, is shown here (arbitrary units). (b) Numerical computation of same quantity taking viscosity into account (from Ogilvie 2005).

2 Experiments

2.1 Experimental set-up

Fig. 4 shows the fully enclosed rectangular container (10 x10 x20 cm^3) as viewed from the top. This container, of square cross-section, was put on a platform and is here shown in its horizontal position (bottom and top perpendicular to direction of rotation axis). The tank is filled with homogeneous, degassed tap water. Via connecting tubes (of diameter d=0.8 cm), water is pumped through the tank by a pump (green in Fig. 4) and flows in the direction indicated by the white arrow, at an imposed rate q [l/min]. Here, $q=0.4572\ V_q + 0.0639$, where V_q is the applied pump voltage (in volts, varying from 0.25-7.0V). Pressure differences are measured with the LPM5480 differential pressure sensor (Druck), which can measure up to ±200 Pa, with a precision of ±0.08 Pa, between pressure slots which are indicated by numbers 1-6 in Fig. 4. Here we focus on the pressure difference between slots 5 and 6, $\Delta p_{5\text{-}6}$. The flow rate is measured by a propeller vane (Höntzsch, Fa 40/10), the device indicated by the red arrow on the left. The platform is set into rotation at an angular velocity ±Ω [rad/s] by a KMF WD251 electromotor (Electro ABI, not visible - below turntable). Here, $\Omega=1.004V_\Omega-0.2942$, where V_Ω (in volts, varying from 0.25-7.0V) is the voltage applied to rotate the turntable.

Automatic control of applied pump and rotation rates, over prescribed measurement T_m and adjustment period T_a respectively, as well as measurement at a 4 Hz rate of differential pressure and flow rate, is made by means of software package *LabView*. In a typical mode of operation, choosing an adjustment period T_a=50 s and a measurement period T_m=150 s, a scan is made over the indicated pump and rotation voltage ranges. This means that at a fixed pump rate, the rotation rate is kept fixed over 200s, of which the final 150 s are used to measure differential pressure and flow speed. Then, the rotation rate is increased by an increment (0.2 or 0.25V) and

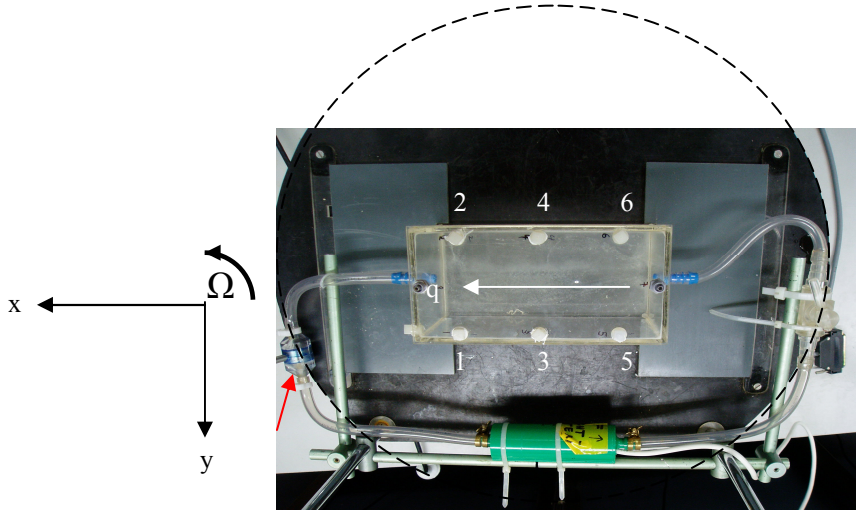

Fig. 4 :Topview of turn table (dashed), container, pump (green), propeller vane (red arrow) and pressure slots1-6

this is repeated until maximum rotation rate is obtained. Subsequently, the flow rate is increased in similar increments, and the rotation rate is incrementally decreased until the lowest rotation rate is reached again, upon which the flow rate is increased again.This whole procedure is then repeated a number of times. The spin-up time needed to adjust to the new frame rotation rate is as usual estimated by $T_E = \Omega^{-1} E^{-1/2}$, where $E = \nu / \Omega H^2$ denotes the Ekman number, ν viscosity and H the (axial) depth of the fluid (Greenspan and Howard 1963). The adjustment period, T_a, that we employ is generally slightly shorter than T_E, but the measured pressure difference has usually adjusted quite well within this period of time.

2.2 Results

When the container is horizontal, we measure a pressure difference whose average over period T_m is given for each bin in figure 5. The table is rotating anticlockwise. We thus expect that the Coriolis force deflects the through flow to the right, so that (see figure 4) the pressure at slot 6 should be increased relative to that at slot 5. As figure 5 presents the pressure at slot 5 minus that at 6, this is indeed observed in the triangular area to the right of the straight solid line; that is, for relatively strong rotation. In this region, we see that the pressure difference is nearly constant (color contours) along hyperbola (curved solid lines). This betrays a *geostrophic equilibrium* in which cross-channel pressure gradient $dp/dy = -2 \Omega u \rho$, so that for a fixed lateral pressure gradient, velocity u is inversely proportional to rotation rate Ω. Here ρ is the density of the fluid. The straight solid line is a line for which the Rossby number, $Ro = U/2\Omega L$, is a constant, whose value depends on the velocity and length scales, U and L, that we adopt (see below). The part above the straight line consists of a positive 'ridge' (red), and an anomalous negative pressure difference. The interruption of the latter region at u=4mm/s is not an artefact. It is found repeatedly in this region and betrays the presence of multiple equilibria, which are reached depending on whether the rotation rate is incrementally increased or decreased. Physically, it is caused by the presence of an eddy. After spin-up to a new rotation rate, the container is usually filled with two vortices: one big cyclonic vortex that fills almost the entire container, and a smaller anticyclonic one. The latter sits near the entrance of the container, on the low-pressure side (in this case below slot 5, to the left of the through-flow) and seems to cause the anomaly. The flow in the container is considered a ‘sheet’ rather plug flow. We regard its lateral extent to be set by the diameter of the feeding tube, d, as rotation prohibits radial

spreading. Its vertical scale, however, seems to be determined by fluid depth, H, as spreading in the axial (vertical) direction is *not* suppressed by the rotation of the frame. Hence as velocity scale we adopt U=q/Hd.

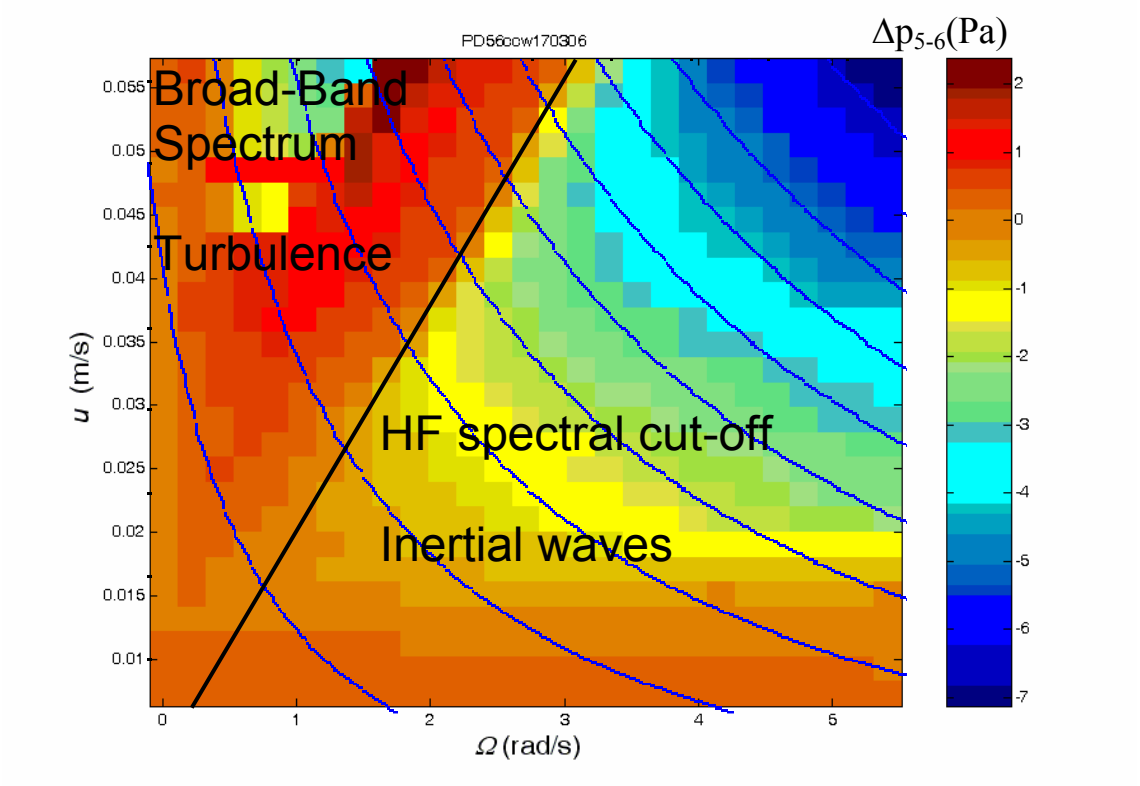

Fig. 5 Each bin represents observed (over a 150s time-interval) averaged pressure difference between slots 5 and 6, $\Delta p_{5\text{-}6}$ [Pa], measured by varying rotation rate Ω and pump rate q. Pump rate is here expressed as velocity of a 'sheet' flow: u=q/Hd, i.e. pump rate q divided by fluid height, H, times jet width, d. The pump rate q is the one found in the absence of rotation, which is linearly related to the applied pump voltage. The straight solid line divides regions having different spectral shape, discussed in the text. Hyperbola reflect geostrophic equilibrium flow, in which, for fixed lateral pressure gradient, through flow is inversely proportional to rotation rate.

The Rossby number associated with the straight solid line in Fig. 5 gets very small when we assume the length scale L to be set by container depth H. However, by considering in each bin the Fast Fourier Transform (power spectrum) of the differential pressure (see example in Fig. 6), we deduce that this length scale L must be diameter d. This conclusion is based on a remarkable change in spectral distribution that takes place across this line. For slow rotation and high pump rates (above straight line in Fig. 5), the variance spreads out equally, indicative of turbulence. However, for fast rotation (below straight line), the power spectrum shows significant variance only below 2 Ω, indicative of inertial waves (Fig. 6c). In a rotating frame, turbulence and inertial waves are considered to take place above and below Ro=1, respectively. Hence we deduce that the straight line should be Ro=1, and we check that along this line, $U/2\Omega=0.056/(2\times3.1)=0.009m \approx d$. In view of the use of the small length scale employed, the relevant Rossby number appears to be a *micro* Rossby number. We conclude that the line Ro=1 separates a hyperbolic regime (Ro<1, below line), where the variance ('turbulence') is taking shape in the form of a 'sea of inertial waves' (Tritton 1978), from a weakly-rotating 'elliptic' region (Ro>1, above line), where variance appears as a spectrally broad-band phenomenon, such as turbulence in non-rotating fluids.

In the Ro<1 (inertial wave) regime, the low-frequency variance is often particularly present near ω=Ω. This is probably due to a slight misalignment of the table's rotation axis with gravity (see peak near ω/2Ω=1/2 in Fig. 6b). This is not the only spectral peak though, and a host of instability processes may be responsible for them (Greenspan 1968, Finlay 1992).

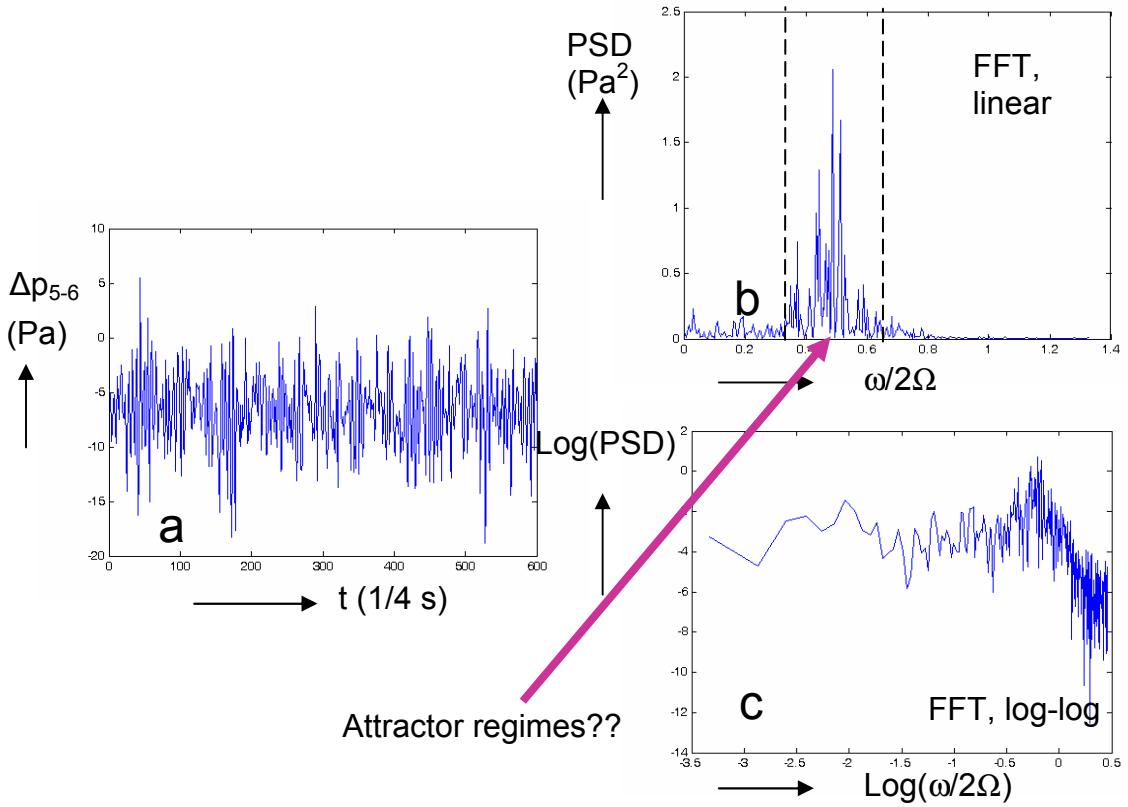

Fig. 6 (a) Example of differential pressure (150 s) time series measured at 4 Hz, $\Delta p_{5\text{-}6}$, whose time average is shown in a single bin in Fig. 5. (b) Its power spectral density (PSD) as function of scaled frequency ω/2Ω in linear and (c) log-log representation. Here V_Ω=5 V, V_q=4 V, and tilt is 10°. Dashed lines in (b) indicate solid bar in Fig. 2a.

When the tank is tilted, the power contained in very low frequency waves (ω/2Ω<0.1) is large, and manifests itself close to the line Ro=1. In Fig.7a, this line is nearly diagonal. It is slightly less steep as the corresponding one in Fig. 5, because under tilt the axial extent of the jet is increased to H/cos(θ), reducing the speed corresponding to a given flow. The increase of low-frequency power along this line can be seen in Fig. 7a, where the percentage of the variance contained in this band relative to total variance is given. In a movie, clear cyclonically propagating waves are observed. The movie's interpretation is facilitated by noting that due to the tank's tilt, the depth of the fluid as measured along the direction of the rotation axis decreases towards the corners on either side (Fig. 8). This provides for the stretching and shrinking of vortex tubes which supports low-frequency topographic Rossby waves. Fig. 7b shows direct evidence of the Rossby wave's strong presence, having a period of 18s, or about 20 rotation periods.

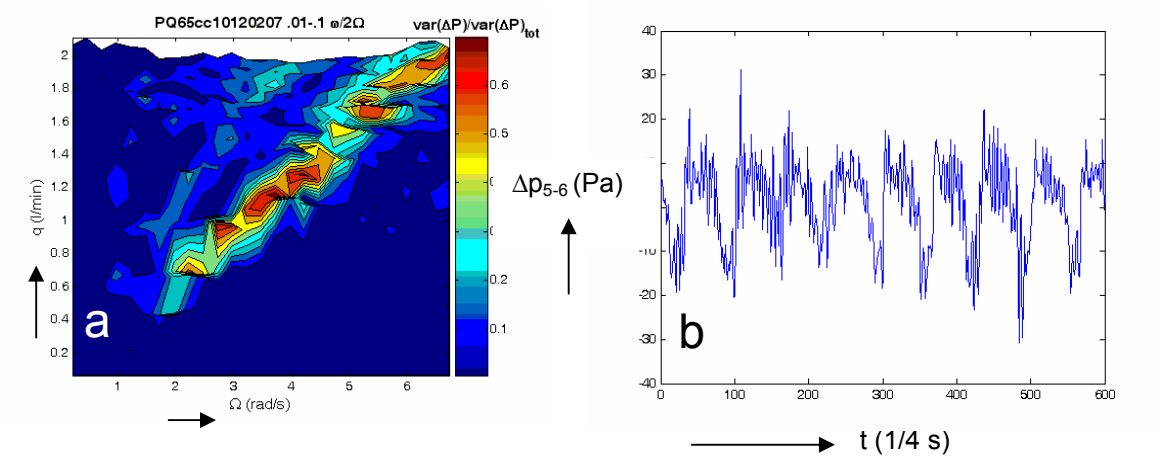

Fig.7 (a) Fraction of low-frequency ($\omega/2\Omega<0.1$) power relative to total variance; (b) example of pronounced low-frequency time variations (measured at 4 Hz) in lateral pressure difference for $V_\Omega=7$ V, $V_q=6.75$ V, corresponding to a point near upper right corner in (a) and tilt angle equal to 10^o.

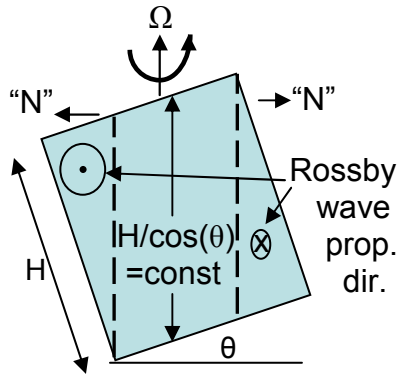

Fig. 8 Sketch of tilted rectangle, showing two triangular regions with vortex tube compression, where the Rossby wave restoring mechanism works. Note that the classical association in geophysical fluid dynamics of the shallow parts indicating "North" is here shown to lead to two "N" directions

The question that concerns us here is whether the inertial waves, once excited, support the through flow. One might expect this from (a) the observed overlap of the frequency window of waves that are excited (in between the dashed lines in Fig. 6b) with the regime for which, according to Fig. 2a (solid line segment), a simple wave attractor exists, and (b) the fact that the presence of a simple attractor was observed to facilitate the generation of a mean flow (Maas 2001), which may possibly be of relevance here for the excitation of both a time-averaged recirculation as well as through flow. For this reason, let us look at observed flows obtained from (1) the horizontal rotating tank compared to the non-rotating tank (Fig. 9a), and (2) the tilted rotating tank compared to the horizontal (non-tilted) rotating tank (Fig. 9b,c). In case 2, the tank is tilted 10 and 20 degrees respectively. In Fig. 9, the *measured* through flow is denoted Q, to distinguish it from the intended through flow q, set by V_q. Note, in the nonrotating case Q ≡q.

Surprisingly, even in the non-tilted case (Fig. 9a), rotation seems to enhance the through-flow, particularly in the rapidly rotating triangular (Ro<1) region of the parameter plane spanned by the rotation rate (x-axis) and pump rate (y-axis). For Ro<1, a further enhancement is found over that already present when the tank is tilted (Fig. 9b, c), with the exception of the region where the pump speed is small, for which the through flow is instead obstructed.

3 Discussion

For high rotation rate, the average cross-channel pressure difference is found to be in near-geostrophic balance. Judging from the spectral distribution of differential pressure, the perturbations in this area take the form of inertial waves. This inertial wave regime can be interpreted as the region where Ro<1. This interpretation requires Ro to be identified with a micro Rossby number, for which velocity scale is that of a sheet flow and length scale is set by that of the connecting tube. For low pump rates, perturbations are concentrated around certain spectral peaks (notably Ω). For higher pump rates, the spectrum is broader (albeit always staying well below the inertial frequency cut-off, 2 Ω). The 3D turbulent regime is found for Ro>1. While for Ro>1 the naïve expectation that rotation will inhibit the through flow, is in general found to be true, this is surprisingly not so in the inertial wave regime (Ro<1). Apart from the enhancement already found when the container is still in its flat position, perhaps due to a tilt of the *effective* rotation vector due to the presence of vertically sheared mean flow (hence creating an *apparent* tilt of the tank), a further enhancement is observed when the tank is itself tilted, especially when the pump rate is relatively large (and the spectrum broad-banded). We speculate that the latter enhancement is brought about by the organization of inertial waves. For some of these frequencies they will be focused onto a simple shaped wave attractor, where, as was found in an earlier study (Maas 2001), they mix background angular momentum leading to the generation of a cyclonic mean flow. It is speculated that for large flow rates, the

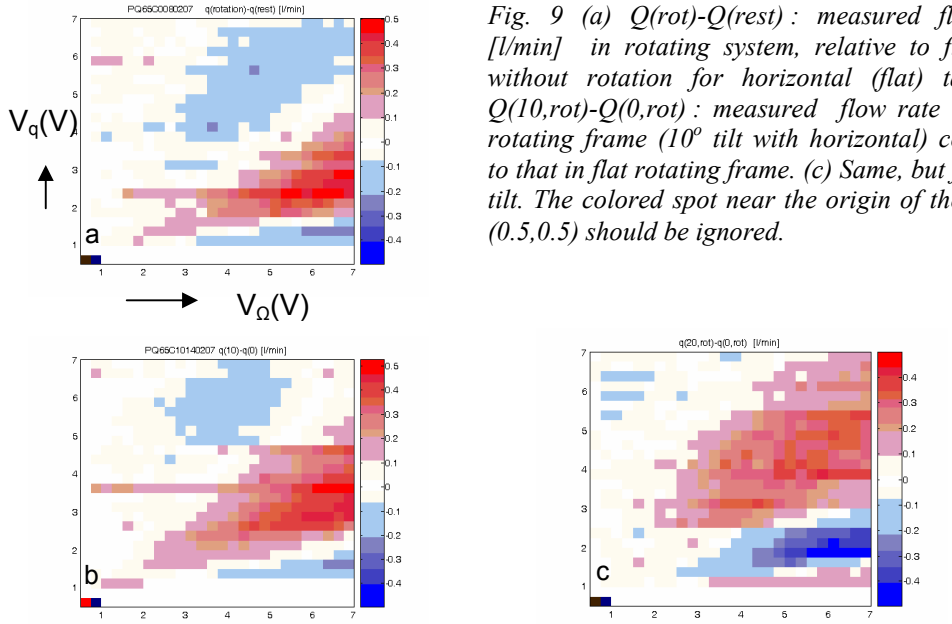

Fig. 9 (a) Q(rot)-Q(rest) : measured flow rate [l/min] in rotating system, relative to flow rate without rotation for horizontal (flat) tank. (b) Q(10,rot)-Q(0,rot) : measured flow rate in tilted, rotating frame (10^o tilt with horizontal) compared to that in flat rotating frame. (c) Same, but for a 20^o tilt. The colored spot near the origin of the graphs (0.5,0.5) should be ignored.

broad-band spectrum encompasses those frequencies for which a wave attractor can be obtained and thus a mean and through flow is driven, while for small pump rates the few frequencies observed are likely not inside an attractor window, so that they only lead to extra damping, reducing the through-flow. Further analysis is needed to substantiate these speculations.

Acknowledgements

The author wishes to thank the organizer of the 2007 St. Petersburg 'Fluxes and Structures in Fluids' conference, Prof. Yuli D. Chashechkin, for his kind invitation to participate. He is also grateful to Niels Smit and Maurits Kruijt for help with the experiments and to Stefan Kopecz for providing Fig. 1. Special thanks also to Astrid Manders for preparing Fig. 3a and to the Fluid

Dynamics group of Eindhoven Technical University, for their hospitality, enabling the experiment of Fig. 3a. Finally, the author is grateful to Uwe Harlander and Louis Gostiaux for insightful comments on the manuscript.

References

Bewley, G., Lathrop, D.P., Maas, L.R.M. and K.R. Sreenivasan, 2007 Inertial waves in rotating grid turbulence. *Phys. Fluids* **19**, 071701

Davidson P.A., Staplehurst P.J. and S.B. Dalziel 2007 On the evolution of eddies in a rapidly-rotating system *J. Fluid Mech*. (submitted)

Dobner, E. 1959 Über den Strömungswiderstand in einem rotierenden Kanal, *Dissertation*, Technische Hochschule Darmstadt.

Finlay, W.H. 1992 Transition to turbulence in a rotating channel. *J. Fluid Mech*. **237**, 73-99.

Greenspan, H. P. 1968 The theory of rotating fluids. *Cambridge University Press*

Greenspan, H.P. and L.N. Howard 1963 On a time dependent motion of a rotating fluid. *J. Fluid Mech.* **17**, 385-404

Maas, L.R.M. 2001 Wave focusing and ensuing mean flow due to symmetry breaking in rotating fluids *J. Fluid Mech.* **437**, 13-28

Maas, L.R.M. 2003 On the amphidromic structure of inertial waves in a rectangular parallelepiped. *Fluid Dyn. Res*. **33**, 373-401

Maas, L.R.M. 2005 Wave attractors: linear yet nonlinear. *Int. J. Bifurc. & Chaos* **15**, 2757-2782

Maas, L.R.M. and F.-P. A. Lam, 1995 Geometric focusing of internal waves. *J. Fluid Mech.* **300**, 1-41

Maas, L.R.M., Benielli, D., Sommeria, J. and F.-P.A. Lam 1997 Observation of an internal wave attractor in a confined stably-stratified fluid. *Nature* **388**, 557-561

Manders, A.M.M. and L.R.M. Maas 2003 Observations of inertial waves in a rectangular basin with one sloping boundary. *J. Fluid Mech.* **493**, 59-88

Manders, A.M.M. and L.R.M. Maas 2004 On the three-dimensional structure of the inertial wave field in a rectangular basin with one sloping boundary. *Fluid Dyn. Res*. **35**, 1-21

Mårtensson G.E., Gunnarsson J., Johansson A.V. and H. Moberg 2002 Experimental investigation of a rapidly rotating turbulent duct flow. *Exp. fluids* **33**, 482-487

McGuinness D.S., Boyer D.L. and H.J.S. Fernando 2001 A laboratory study of mean flow generation in rotating fluids by Reynolds stress gradients *J. Geophys. Res.* **106**, 11691-11707

Messio, L, Morize, C., Moisy, F. and M. Rabaud, 2007 Experimental observation using particle image velocimetry of inertial waves in a rotating fluid. *Exp. in Fluids* (in press).

Morize C. and F. Moisy 2006 Energy decay of rotating turbulence with confinements effects. *Phys. Fluids* **18**, 065107

Nandakumar, K., Raszillier, H. and F. Durst 1991 Flow through rotating rectangular ducts. *Phys. Fluids* A**3**, 770-781

Ogilvie, G. 2005 Wave attractors and the asymptotic dissipation rate of tidal disturbances. *J. Fluid Mech*. **543**, 19–44

Pallares, J., Grau, F.X. and L. Davidson 2005 Pressure drop and heat transfer rates in forced convection rotating square duct flows at high rotation rates *Phys. Fluids* **17**, 075102

Phillips, O.M. 1963 Energy transfer in rotating fluids by reflection of inertial waves. *Phys. Fluids* **6**, 513-520

Swart, A.N. 2007 Internal waves and the Poincaré equation. *Ph.D. thesis Utrecht University*

Thompson, R.O.R.Y. 1970 Diurnal tides and shear instabilities in a rotating cylinder *J. Fluid Mech*. **40**, 737-751

Tritton, D.J. 1978 Turbulence in rotating fluids. *From:* Rotating fluids, *eds*. P.H. Roberts and A.M. Soward. *Ac. Press,* 105-138